Direct Imaging of Dehydrogenase Activity within Living Cells Using Enzyme-Dependent Fluorescence Recovery after Photobleaching (ED-FRAP)

C. A. Combs and R. S. Balaban
Laboratory of Cardiac Energetics, National Heart, Lung, and Blood Institute, National Institutes of Health, Bethesda, Maryland 20892-1061 USA

ABSTRACT Reduced nicotine adenine dinucleotide (NADH) is a key metabolite involved in cellular energy conversion and many redox reactions. We describe the use of confocal microscopy in conjunction with enzyme-dependent fluorescence recovery after photobleaching (ED-FRAP) of NADH as a topological assay of NADH generation capacity within living cardiac myocytes. Quantitative validation of this approach was performed using a dehydrogenase system, in vitro. In intact cells the NADH ED-FRAP was sensitive to temperature (Q_{10} of 2.5) and to dehydrogenase activation by dichloroacetate or cAMP (twofold increase for each). In addition, NADH ED-FRAP was correlated with flavin adenine dinucleotide (FAD^+) fluorescence. These data, coupled with the cellular patterns of NADH ED-FRAP changes with dehydrogenase stimulation, suggest that NADH ED-FRAP is localized to the mitochondria. These results suggest that ED-FRAP enables measurement of regional dynamics of mitochondrial NADH production in intact cells, thus providing information regarding region-specific intracellular redox reactions and energy metabolism.

INTRODUCTION

The regulation of many cellular processes is thought to be influenced by the regional distribution of enzymes and local conditions (Srivastava and Bernhard, 1987; Saks et al., 1991). The study of cellular compartmentation has generally been limited to evaluating the intracellular distribution of enzymes/proteins/metabolites or the imaging of regional ionic conditions. A recent study has shown direct visualization of enzymatic processes in living cells using fluorescence resonance energy transfer (FRET) on GFP-modified proteins (Nagai et al., 2000); however, quantification of enzyme activity from regions within living cells has not been reported. A method for measuring enzymatic activity in vivo would assist in integrating regional cytosolic regulatory processes. We hypothesized that the recovery of fluorescence of a fluorophore after photobleaching could be used to assay regional intracellular enzymatic activity. In this study we have focused on the regeneration of the reduced form of nicotinamide adenine dinucleotide (NADH) in the cell due to its key role in cellular metabolism.

Fluorescence recovery from photobleaching (FRAP) has been extensively used to measure translational mobility of various fluorophores. This technique involves the photobleaching of a fluorophore and observing the kinetics of the fluorescence recovery dependent on passive diffusion and active translational processes (protein transport) (Axelrod et al., 1976; Icenogle and Elson, 1983; Smith et al., 1998). We proposed that the motion effects in FRAP could be eliminated by bleaching the entire cell, and be made dependent on enzymatic activity through the resynthesis of the fluorophore pool after photobleaching. This approach would result in an enzyme-dependent fluorescence recovery after photobleaching (ED-FRAP).

Conveniently, the NAD^+/NADH ratio is large in most cells (Erecinska et al., 1978), reducing the impact of the NADH photobleaching on the total NADH-NAD^+ cellular content. In addition, the intrinsic NADH fluorescence signal from cells is a good candidate for ED-FRAP because this molecule plays a critical role in energy metabolism and numerous other redox coupled reactions in the cell (Chance et al., 1972; Eng et al., 1989). The dehydrogenases that generate NADH are highly regulated and compartmentalized enzymes involved in the effects of hormone action (McCormack et al., 1990), as well as the orchestration of workload with oxidative phosphorylation (Balaban, 1990). To date, the cellular activity of dehydrogenases has been extrapolated, indirectly, from NADH fluorescence amplitude images. These studies cannot discriminate between a change in NADH production and NADH utilization resulting in the net change in [NADH]. This is a general problem for cellular fluorescence measurements of metabolic intermediates. Here we show that ED-FRAP can provide a direct measure of dehydrogenase activity, removing the ambiguity of interpreting NADH fluorescent amplitude changes with experimental perturbations.

Received for publication 13 September 2000 and in final form 22 January 2001.

Address reprint requests to Dr. Christian A. Combs, Laboratory of Cardiac Energetics, National Heart Lung and Blood Institute, National Institutes of Health, Bldg. 10, Rm. B1D-416, Bethesda, MD 20892-1061. Tel.: 301-496-0014; Fax: 301-402-2389; E-mail: combsc@zeus.nhlbi.nih.gov.

0006-3495/01/04/2018/11 $2.00

METHODS

Preparation of cardiac myocytes and mitochondria and experimental conditions

Cardiac myocytes were isolated from adult rabbits using standard procedures (Chacon et al., 1994). Cells were resuspended after isolation in media

consisting of a 1:1 mixture of Joklik's medium and medium 199 supplemented with 1 mM creatine, 1 mM carnitine, 1 mM taurine, 1 mM octanoic acid, 10 mM Hepes, 5 mM hydroxybutyric acid, 0.05 units/ml insulin, 10 units/ml penicillin, and 10 μg/ml streptomycin at pH 7.4. Cells were plated onto coverslips coated with Matrigel (Becton, Dickinson, Franklin Lakes, NJ) for attachment before each experiment. All experiments were conducted within 8 h of isolation. Mitochondria were isolated as previously described (Territo et al., 2000). Temperature was maintained at 37°C in some experiments by blowing heated air from a commercial air-heating system (World Precision Instruments Inc., Sarasota, FL) into a custom-built box surrounding the microscope and by using a heated sample chamber (Warner Instruments, Hamden, CT). Superfusion through the sample chamber was performed by gravity-feed.

Glutamate dehydrogenase enzyme system

Equilibrium conditions were produced by mixing 5 mM α-ketoglutarate, 5 mM NAD^+, 1 mM glutamate, 50 mM Tris, and 300 μM NH_4^+ at pH 8.0 with varying amounts of glutamate dehydrogenase (Lowry and Passonneau, 1972). Using an equilibrium constant of 4.5×10^{-14} M^2 (Barman, 1969) the [NADH] was estimated at 1.5 μM. Borosilicate pipettes drawn to a tip of $\cong$5 μm were used to produce the micro-droplets. All experiments were conducted under silicone oil to avoid evaporation.

Image acquisition and data analysis

All fluorescence emission images of micro-droplets and cardiac myocytes were obtained with a Zeiss LSM-510 confocal microscope system. Images of the droplets were collected with a Fluar 10×, 0.5 NA lens. Images of the isolated mitochondria and the cardiac myocytes were collected with a C-Apochromat 63×, 1.2 NA, water lens. In all cases the center of the cell or droplet was selected to image and the pinhole adjusted to produce a thin slice (1.4–2.0 μM in cells and mitochondria and 85 μM in the droplets). NADH was imaged with the 351-nm line of a UV laser and an LP 385-nm emission filter (Eng et al., 1989). Flavin adenine dinucleotide (FAD^+) was imaged using the 488-nm line of an argon laser and a BP 505–550 nm emission filter (Chance et al., 1972). All image processing was performed using custom-written programs written in the IDL programming environment (RSI, Boulder, CO).

RESULTS

In vitro ED-FRAP validation

To validate the ED-FRAP approach, experiments were conducted on small droplets ($\sim$350 μm diameter) with glutamate dehydrogenase (GDH) in an equilibrium mixture of its substrates including NADH ($\sim$1.5 μM). The photobleaching was accomplished by bleaching the entire droplet (at 351 nm) to eliminate motion effects in the fluorescence recovery. Images of an enzyme containing droplet before, immediately after photobleaching, and after recovery are shown in Fig. 1 *A*. An example of the time course of fluorescent recovery is presented in Fig. 1 *B*. Droplets that contained NADH in water alone without the enzyme reaction components were found to bleach uniformly, but not recover.

To quantify the NADH recovery rate versus enzyme concentration we assumed that the exponential recovery of NADH fluorescence is a reversible pseudo-first-order reaction ($NAD^+ \leftrightarrow$ NADH) that re-establishes steady state after photobleaching according to the equation:

$$\mathrm{NADH} = \mathrm{NADH_{eq}} + (\mathrm{NADH_b} - \mathrm{NADH_{eq}})(e^{-k_{\mathrm{NADH}}\tau}).$$

Where k_{NADH} is the sum of the forward (k_f) and reverse (k_r) rate constants of the pseudo-first-order reaction, $\mathrm{NADH_b}$ is the initial fluorescence intensity after photobleaching, τ is the time after photobleaching, NADH is the fluorescent intensity, and $\mathrm{NADH_{eq}}$ is the steady-state NADH fluorescence signal after bleaching. The assumption that the recovery was exponential was supported by the observation that the recovery rate could be fit to Eq. 1 (Chi-square, $p < 0.05$). Because this reaction is enzyme-catalyzed, the observed forward and reverse rate constants will be dependent on the enzyme concentration (i.e., $k_{\mathrm{NADH}} = [E]k_f + [E]k_r = [E](k_f + k_r)$). Thus, k_{NADH} should be proportional to the enzyme concentration in a pseudo-first-order rate reaction. The calculated k_{NADH} value was found to be proportional to [GDH] ($R^2 > 0.99$) in the droplets (Fig. 1 *C*). Varying the degree of bleaching with light intensity or time did not significantly change the k_{NADH} value for a given enzyme concentration. The initial rate under these conditions (1.5×10^{-10} mol/min/Unit Enzyme), estimated from the initial linear region of the ED-FRAP recovery curve, indicated that the enzyme was operating well below $V_{\max}$ due to the concentrations of metabolites used in this steady-state experiment (Barman, 1969), as well as the fact that true initial rate conditions might not have been obtained (i.e., incomplete photobleaching of NADH).

Effect of steady-state fluorescence imaging on living myocytes

In previous studies using bright field microscopy, we found that the NADH fluorescence signal is dominated by the mitochondrial pool and that a slow decline in signal was observed over time (Eng et al., 1989). In the current study using confocal techniques, we observed a similar dynamic phenomenon with imaging time. An initial decay in NADH fluorescence was observed followed by an extended steady state that was stable for hundreds of more images (Fig. 2). This result suggested that a new steady state of NADH was being created by the imaging procedure. This was likely due to the competition between the optical destruction of NADH with its metabolic production. This hypothesis was tested by pausing the image acquisition and observing the effects on the NADH signal. The results from one of these studies are presented in Fig. 3. When imaging was paused, NADH substantially recovered as metabolism regenerated NADH without the competition of photobleaching. Over time, the NADH signal returned to the original steady-state level. These data are consistent with a balance between the destruction, via photobleaching, and generation, via metabolism, resulting in the observed steady state of NADH during

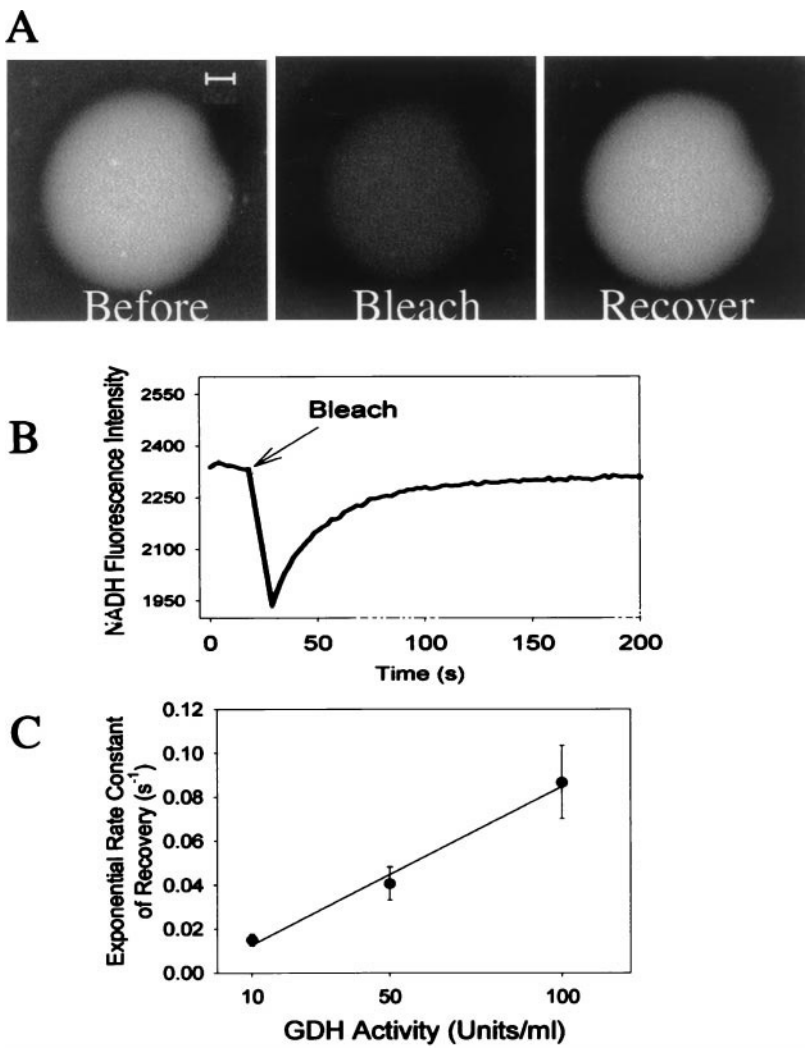

FIGURE 1 NADH recovery is exponential and is enzyme-dependant in vitro. (*A*) NADH fluorescence images (85 μm slice thickness) from a droplet containing 10 units/ml of GDH and substrates in equilibrium before and immediately after the bleach pulse (75 μW, <2 μs dwell time/pixel), and after complete recovery. The scale bar represents 50 μm. (*B*) Representative plot of NADH fluorescence intensity over time during an ED-FRAP experiment from a droplet containing the GDH enzyme system. (*C*) Plot of exponential rate constant (k_{NADH}) for recovery from photobleaching of NADH from droplets containing variable concentrations of GDH. $n = 5$ for each [GDH].

imaging. This steady-state condition also suggests that the photodamage to the NADH generation system is minimal over the time of these experiments, because if the NADH generating capacity was being reduced, the NADH levels would be rapidly reduced by the background photobleaching of the imaging processes itself. Further confirmation that metabolic resynthesis of NADH was occurring is presented in the ED-FRAP experiments that follow.

NADH fluorescence photobleaching recovery characteristics and distribution in living myocytes

Fig. 4 shows an NADH ED-FRAP experiment on a cardiac myocyte. Again, the entire cell was photobleached to eliminate diffusional processes. The cell NADH fluorescence recovered in a similar exponential function as seen in the in vitro enzyme studies consistent with an enzymatic process (Fig. 4, *A* and *B*) and the resynthesis of reduced NADH. The photobleaching was found to pass through the entire cell using the non-metabolized probe, calcein-AM, that demonstrated out-of-plane bleaching using slower 3D imaging procedures (data not shown). This result suggests that through-plane diffusion of NADH was unlikely in these studies. Photobleached cells did not exhibit signs of damage such as blurred z-lines, spontaneous contractions, or blebbing (Fig. 4 *A*). The photobleaching pulse had no direct effect on mitochondrial membrane potential using tetramethylrhodamine methyl ester (TMRE) as a probe (data not shown).

The effect of photobleaching magnitude on the rate of NADH recovery was evaluated serially on individual myocytes. This is presented in Fig. 5 *A*. As seen in Fig. 5, *A* and *B*, the recovery rate of NADH increased with bleaching level (ANOVA, $p < 0.05$). There was an apparent nonlinear (exponential) dependence of the rate of recovery of NADH with the bleaching level as shown in Fig. 5 *B*. These data suggest that the metabolic recovery rate is dependent on the magnitude of the perturbation imposed and suggest that standardized bleaching conditions will need to be used in comparison studies. In addition, because these studies were

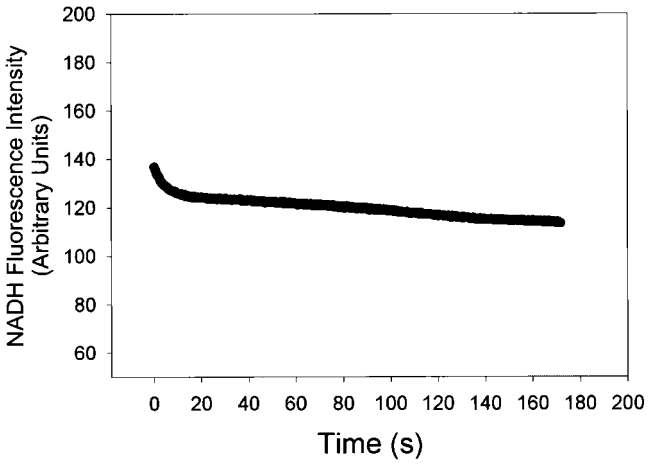

FIGURE 2 NADH fluorescence over time in isolated perfused cardiac myocytes. Representative plot of NADH fluorescence intensity over time at a rate of imaging of 3 Hz. Intensity values are the mean of all pixel values greater than the background fluorescence in the myocyte. Note that there is an initial steep decrease followed by a slow constant decline in fluorescence intensity where NADH bleaching rate is balanced by metabolic generation of NADH.

performed serially in the same myocytes, there is apparently no significant damage to the NADH regeneration system with the bleaching pulse. Indeed, the fact that the highest bleaching level (i.e., highest power) resulted in the fastest recovery rate is also inconsistent with a bleaching-related lesion to the NADH production system.

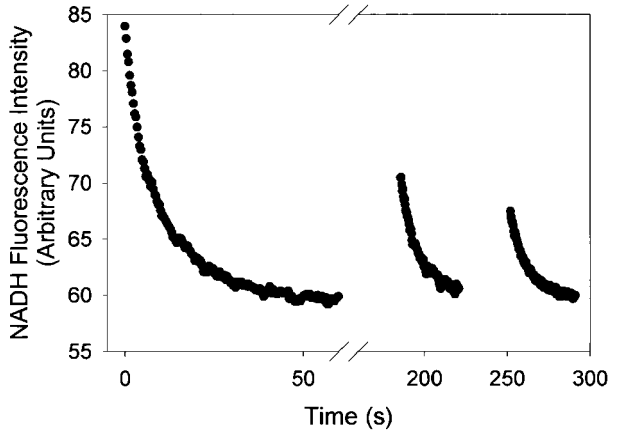

FIGURE 3 Balance between photobleaching and metabolic generation of NADH over time in an isolated perfused cardiac myocyte during image acquisition as evidenced by regeneration of NADH during pauses in the imaging experiment. Plot of NADH fluorescence intensity over time at a rate of imaging of 3 Hz with two pauses. Intensity values are the mean of all pixel values greater than the background fluorescence in the myocyte. Note that NADH substantially recovers during the two pauses and follows an exponential decay similar to the initial decay upon resumption of imaging.

A zoomed region of a myocyte NADH fluorescence image is shown in Fig. 6 *A*. The characteristic fluorescent patterns of mitochondria are observed localized to the regions between the z-lines in the sarcomeres and densely located in the perinuclear regions. Previous studies have established that the mitochondrial NADH fluorescence signal dominates in this preparation (Eng et al., 1989). The mitochondrial NADH signal is large due to concentration and the large fluorescence enhancement associated with protein binding in the matrix (Nuutinen, 1984; Jameson et al., 1989).

The k_{NADH} value was calculated on a pixel-by-pixel basis from an ED-FRAP experiment on this cell to create the activity map in Fig. 6 *B*. This image demonstrates that adequate signal-to-noise was attained to determine the distribution of this process within a single living cell. The activity map shows the highest rates of NADH recovery were localized to the mitochondria. NADH signal from the cytosol (z-line regions) and nucleus were too low to quantify reliably.

To confirm that mitochondria have a significant NADH recovery capacity, ED-FRAP experiments were conducted on isolated porcine heart mitochondria. Fig. 7 shows an NADH ED-FRAP experiment conducted on a dense field of mitochondria at 25°C. The fluorescence recovery in this isolated organelle is clearly observed, consistent with the notion that the NADH ED-FRAP recovery is occurring in the mitochondria. Quantitative comparisons of the mitochondrial k_{NADH} and cellular rates are difficult due to the differences in carbon substrates utilized as well as species differences.

Because the NADH is bound in the mitochondria, intracellular diffusion should not contribute to the NADH recovery even if the whole cell was not irradiated. This was confirmed by obtaining the same k_{NADH} value in a small bleached region (⅓ of the cell) as the whole-cell bleach procedure (not shown). In addition, no evidence of an increase in the NADH signal around a selectively bleached region was observed, consistent with the notion that the mitochondrial NADH is immobilized. One of the concerns in interpreting the mitochondrial NADH ED-FRAP recovery is the fact that NADH immobilization enhances the fluorescence so markedly (Nuutinen, 1984; Jameson et al., 1989). The kinetics of this binding process could contribute to the ED-FRAP rate constant if binding is much slower that the enzymatic rates. The contribution of the binding kinetics will be discussed further below.

Cellular NADH fluorescence photobleaching recovery rate is sensitive to temperature and dehydrogenase activity

To further evaluate whether the NADH ED-FRAP rates in the myocytes were dependent on enzymatic processes, experiments were conducted to examine the effects of tem-

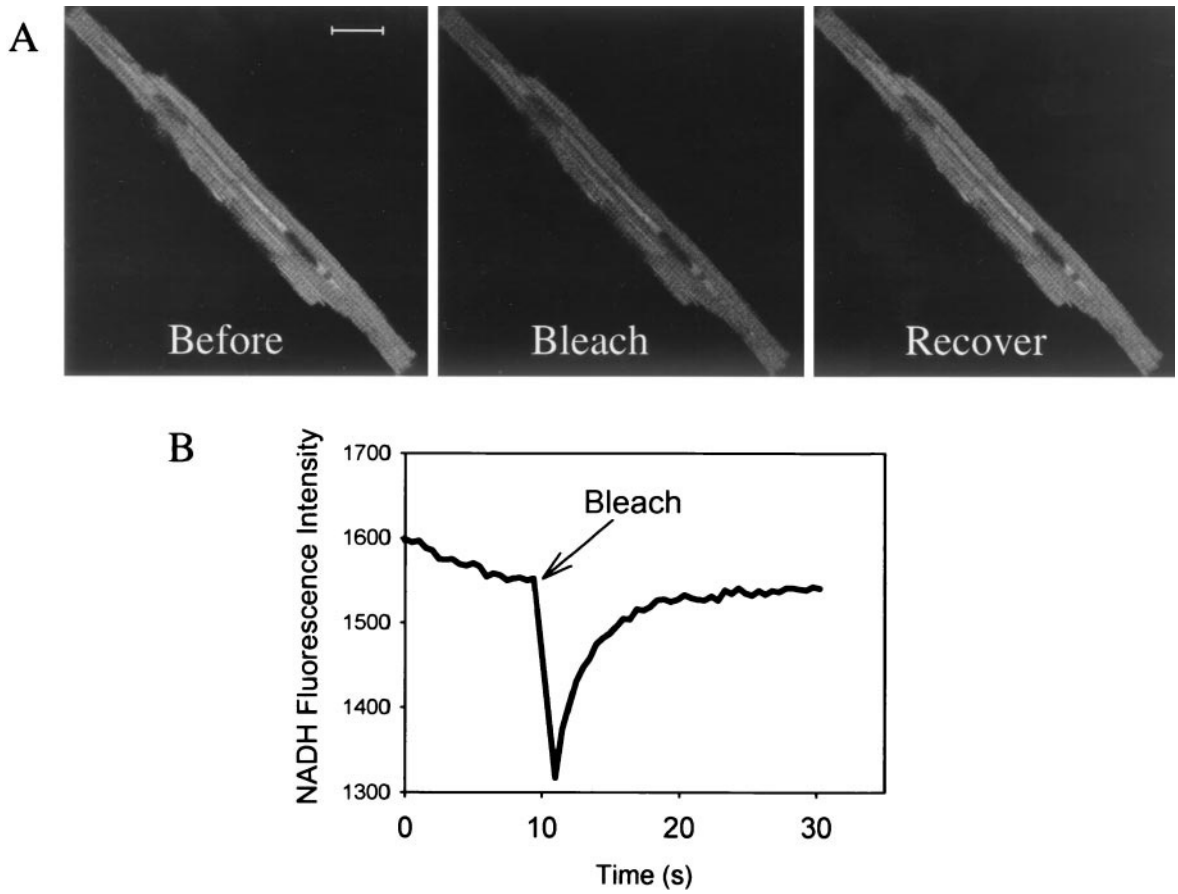

FIGURE 4 NADH fluorescence recovery and cellular viability after photobleaching in isolated perfused cardiac myocytes. (*A*) NADH fluorescence images (2 μM slice thickness) from a myocyte before photobleaching (75 μW, <2 μs dwell time/pixel), immediately after, and following recovery. Obvious structures that can be seen in the cardiac myocyte are the nucleus (large dark spot in the left center) and the z-lines of the sarcomeres (repeating dark lines). The scale bar represents 10 μm. (*B*) Representative plot of NADH fluorescence intensity recovery after a bleach pulse. Intensity values are the mean of all pixel values greater than the background fluorescence in the myocyte. Note that the recovery is exponential and similar to the recovery curve in Fig. 1. .

perature and dehydrogenase activation with dichloroacetic acid (DCA) and cAMP (theophylline) (Bersin and Stacpoole, 1997). Fig. 8 shows the average k_{NADH} value in cardiac myocytes as a function of these treatments. Raising the temperature by 12°C increased the rate by more than a factor of 2.5. This is consistent with the effect of temperature on the activity of most enzymes (Hochachka and Somero, 1984). However, as discussed above, the temperature dependence of NADH binding to matrix proteins could have a similar temperature dependence.

DCA increased average k_f by factors of 3 and 1.5 at 25 and 37°C, respectively. Theophylline was used to simulate hormone activity by increasing cellular cyclic adenosine monophosphate (cAMP) levels. Theophylline increased k_f by 2.5-fold (Fig. 8). These increases in k_{NADH} are similar to the enhancement of pyruvate dehydrogenase activity, determined in vitro, caused by these agents in intact hearts (Bersin and Stacpoole, 1997; Depre et al., 1998). These later data are consistent with k_{NADH} being proportional to the enzyme activity in the mitochondria and not other physical processes, such as NADH protein binding, as it is unlikely that both of these agents would affect NADH binding rates.

The distribution of the effect of DCA is presented in Fig. 6, *C* and *D*, where a reference NADH intensity image (Fig. 6 *C*) and a pixmap of the difference in k_{NADH} values before and after DCA (Fig. 6 *D*) are presented. Fig. 6 *D* shows a clearly punctate pattern of activation by DCA. These changes correlate with the distribution of mitochondria based on NADH fluorescence correlation with mitochondria-specific dyes and metabolic perturbations (Eng et al., 1989). This image demonstrates that adequate signal-to-noise is attained in this approach to image the difference in dehydrogenase activity within a single cell during experimental perturbations.

Effects of NADH photobleaching on FAD^+ fluorescence

Another internal verification of the enzymatic requirement for NADH recovery after photobleaching is the FAD^+

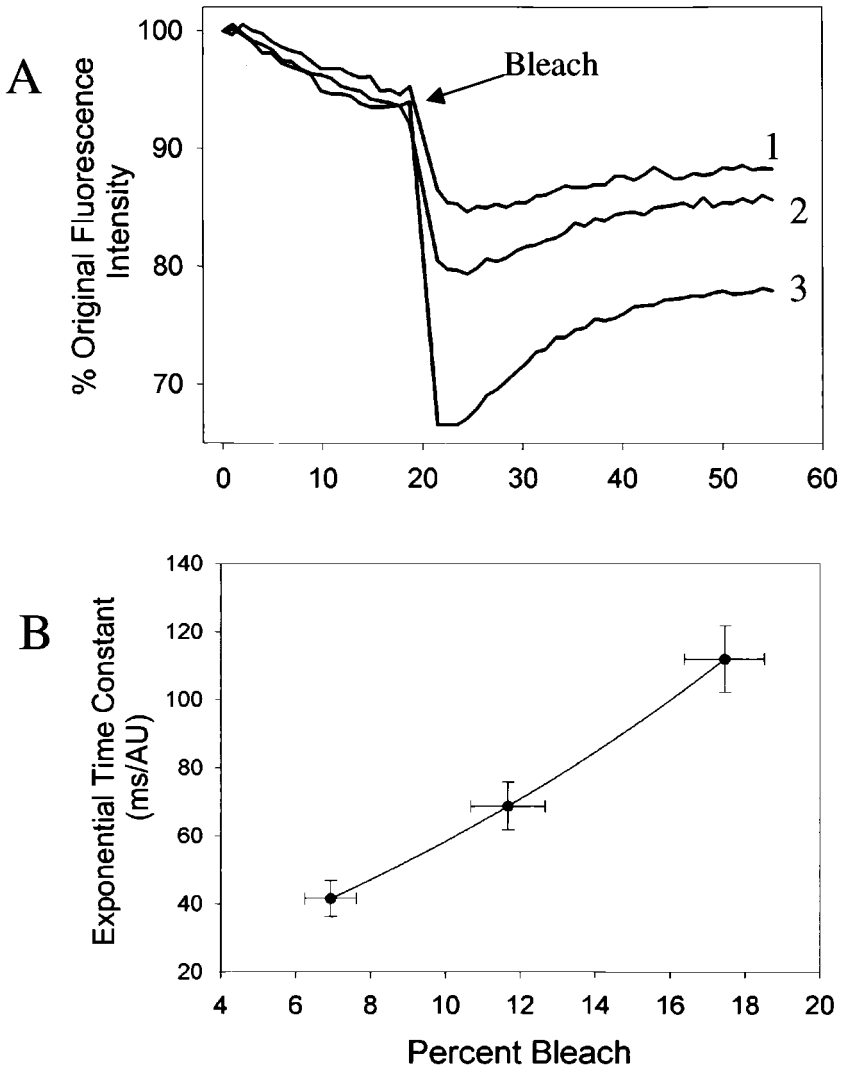

FIGURE 5 Rate of recovery of the autofluorescence of NADH is proportional to bleach level in isolated perfused cardiac myocytes. (*A*) Plots of NADH fluorescence intensity recovery after bleach pulses designed to produce different degrees of photobleaching in repeated measurements on a single myocyte. Intensity values are the mean of all pixel values greater than the background fluorescence in the myocyte. (*B*) Mean and SEM values for the exponential rate constant (averaged over the entire cell volume) of recovery after photobleaching versus treatments designed to produce three different levels of photobleaching (five iterations of ~38 (*curve 1*) or 75 μW (*curve 2*), or 10 iterations of 75 μW (*curve 3*) at a wavelength of 351 nM and a dwell time of 2 μs/pixel) for superfused cardiac myocytes. All bleach levels and recovery rates were significantly different (repeated measures ANOVA, SNK, $p < 0.05$). The line represents an exponential fit of recovery rate versus bleach level ($R^2 > 0.99$).

fluorescence response. FAD^+ and NAD^+ redox states are linked via the NADH ubiquinone reductase, pyruvate dehydrogenase, and other dehydrogenase reactions. Predictably, with NADH depletion, the FADH pool should also be reduced, as it is used to regenerate NADH through these reversible reactions. In contrast to NADH, the oxidized form of FAD^+ is fluorescent, not the reduced form (i.e., FADH), resulting in a decrease in fluorescence intensity with increasing level of FADH (Chance et al., 1972; Kunz and Kunz, 1985; Romashko et al., 1998). Thus, the fluorescence intensities from these two metabolite pools change inversely with increasing reduction level. To test whether the NADH and FAD^+ pools were enzymatically linked, we monitored the NADH and FAD^+ fluorescence signal recovery after a NADH photobleaching pulse in a single cell. An example of these studies is presented in Fig. 9. A transient increase in FAD^+ fluorescence was observed that mirrored the decrease in NADH fluorescence in response to the NADH-directed photobleaching pulse. These data are consistent with the enzymatic coupling of the FAD^+ and NADH metabolite pools as probed using the ED-FRAP approach. Finally, the similar kinetics of FAD^+ enhancement and NADH recovery after NADH photobleaching also suggest that the binding kinetics of NADH to proteins, enhancing the NADH fluorescence signal, are not dominating the NADH fluorescence recovery kinetics.

DISCUSSION

These data demonstrate that NADH ED-FRAP can be used to image the distribution of enzyme-dependent reaction rates in vitro and in intact cells. The correlation between NADH ED-FRAP k_{NADH} and enzyme content (Fig. 1 *C*) confirms that quantitative enzymatic activity can be determined using this approach in vitro. The temperature, DCA, and theophylline sensitivity of the k_{NADH} and the correlation with FAD^+ fluorescence levels found in cardiac myocytes

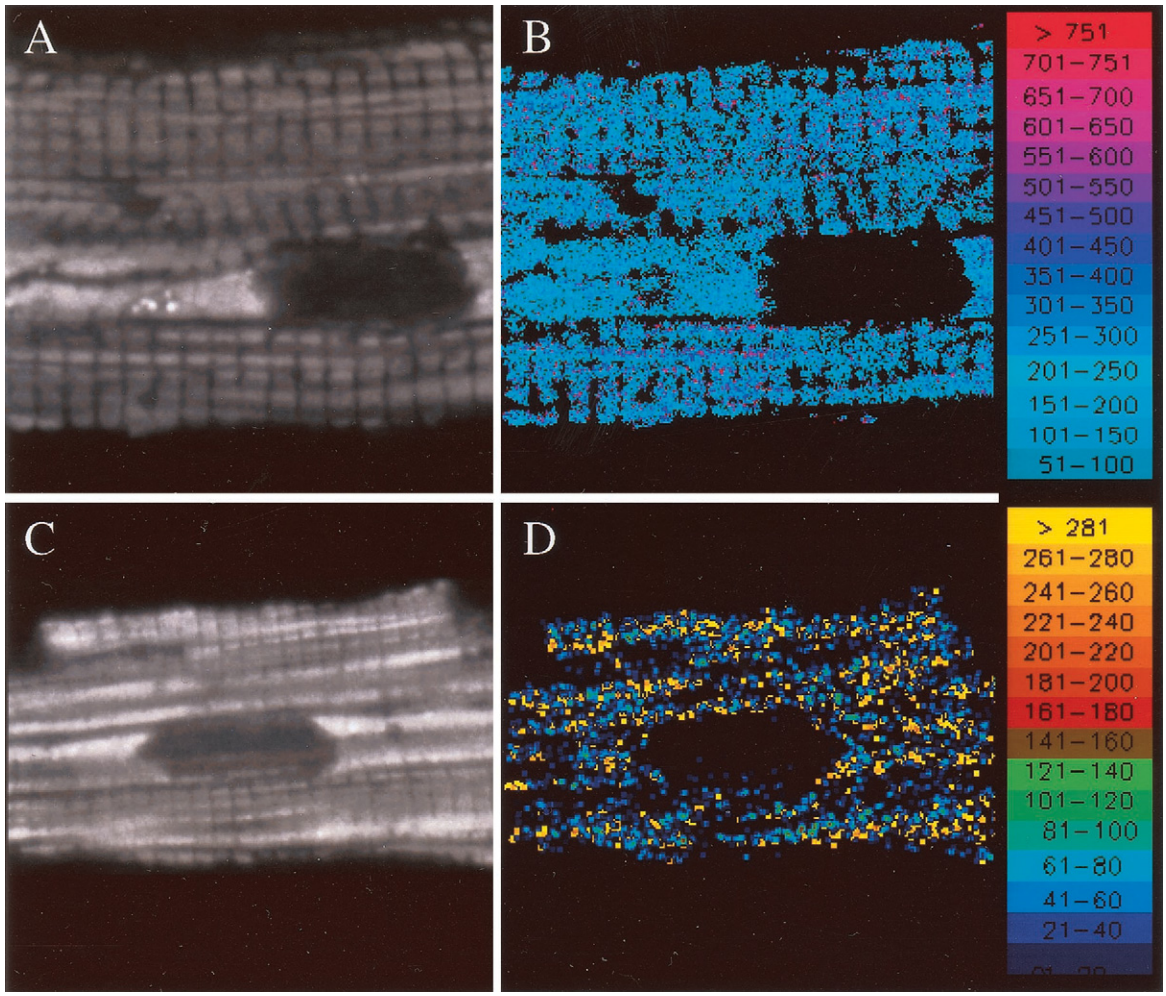

FIGURE 6 Pixmaps of NADH recovery rate reveal regional dehydrogenase activity in isolated cardiac myocytes. (*A* and *C*) NADH fluorescence intensity images (1.5 μM slice thickness). (*B*) False color pixmap of exponential recovery rate $\times 10^{-3}$ s^{-1}. The NADH intensity image was smoothed over two pixels before exponential fitting ($\cong$1 μm in plane and z-resolution). Only pixels that passed a chi-square distribution function were fit. Temporal resolution was 0.49 s for exponential fits. (*D*) Pixmap of the difference in exponential recovery rate between superfusion with nutrient medium and 5 mM DCA of the cell depicted in (*C*). Imaging and photobleaching parameters are the same as in Fig. 1.

support the notion that ED-FRAP is determining the enzyme-dependent NADH generating capacity of regions within the cell.

In this initial study we have not attempted to determine the initial rate of NADH formation (i.e., [E]*k_f) because we have not been able to attain complete removal of the NADH pool with photobleaching. Attempts to perform complete photobleaching with higher power or longer times of irradiation resulted in irreversible cell damage based on gross structural changes. This damage could be due to direct photodamage of the cell or depletion of the total NAD^+/NADH pool as the NADH is rapidly cycled through the reaction and photobleaching process. This latter effect was observed in the enzyme system in vitro with long irradiation times. However, no evidence of direct GDH destruction was observed. We selected a photobleaching level of ~30% in these studies based on empirical observations that this provided a minimal perturbation but adequate signal-to-noise to measure k_{NADH}.

A surprising result was the dependence of k_{NADH} on the bleaching level in the cells, getting faster with larger decreases in NADH (Fig. 5). This was not observed in the isolated enzyme system. The increasing recovery rate with NADH bleaching level suggests that bleaching is not significantly destroying the dehydrogenases, because just the opposite would occur. The fact that the rate of recovery is dependent on the magnitude of the displacement from the steady state could be due to thermodynamic effects on the metabolic driving forces (i.e., NADH/NAD (Wilson, 1994)) or direct negative-allosteric effects of NADH on the dehydrogenases (Patel and Roche, 1990)). These possibilities need to be explored further with regard to the quantitation of ED-FRAP rates and the regulation of cellular NADH production. Without a complete model it is clear that the

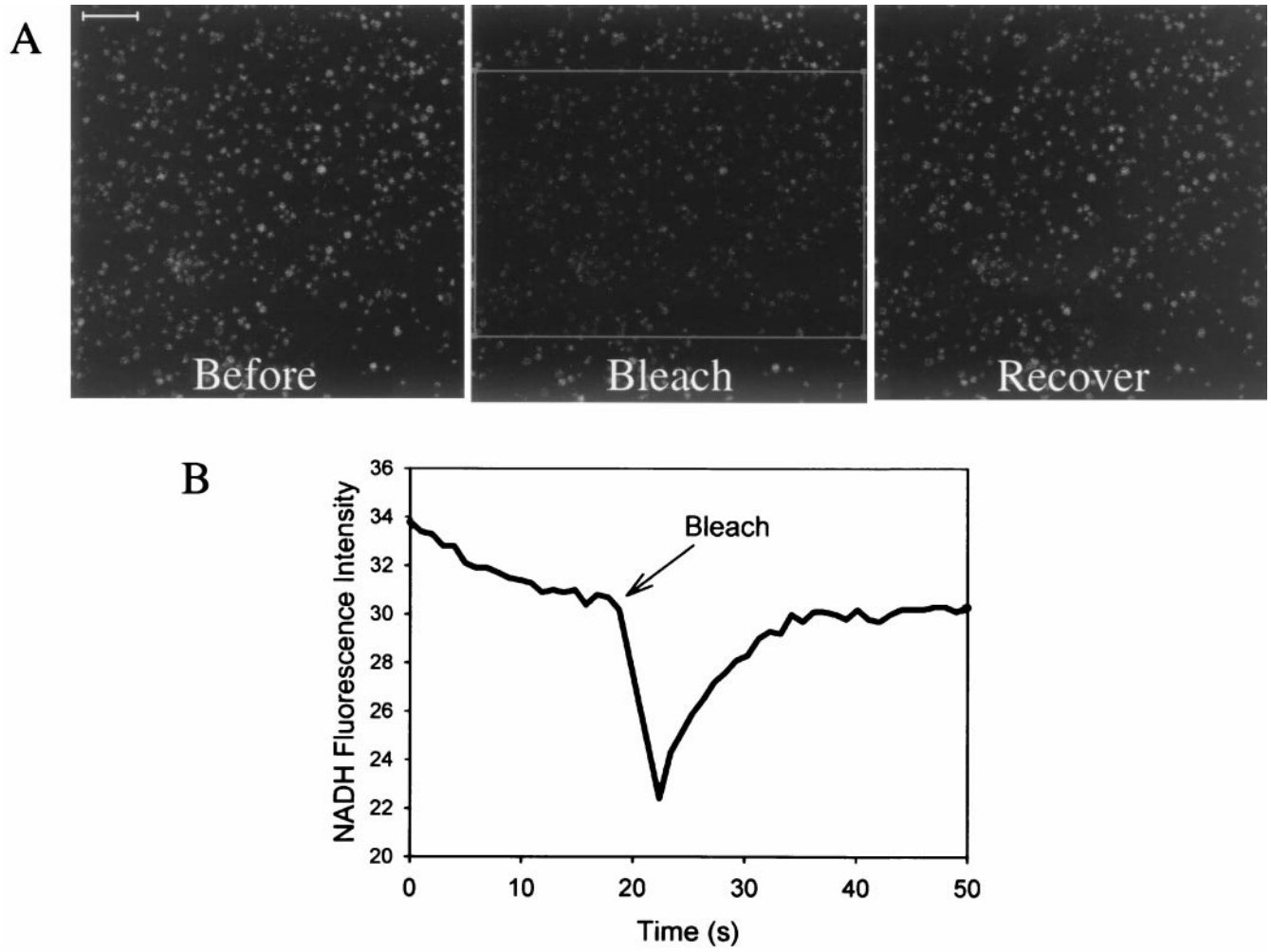

FIGURE 7 NADH fluorescence recovery is exponential in isolated perfused mitochondria. (*A*) NADH fluorescence images (1.4 μM slice thickness) from mitochondria before photobleaching (75 μW, <2 μs dwell time/pixel), immediately after, and following recovery. The box represents the bleaching area. The scale bar represents 10 μm. (*B*) Plot of NADH fluorescence intensity recovery after a bleach pulse. Intensity values are the mean of all pixel values greater than the background fluorescence. Note that the recovery is exponential and similar to the recovery curve in Figs. 1 and 2 .

perturbation, or bleaching level, must be consistent between experimental conditions to access differences in NADH generation capacity.

One other interesting consequence of the NADH ED-FRAP is what it means in the evaluation of NADH using standard fluorescence microscopy techniques. Many investigators have assumed that the bleaching of NADH is minimized in studies where the NADH fluorescence signal is nearly constant or slowly drifts down during an experimental observation period (Eng et al., 1989). However, this apparent constant NADH signal is reflecting the balance between the photobleaching destruction and enzymatic production of NADH described in the current study (Fig. 3). Similar concerns may exist for steady-state fluorescence studies on FAD^+ and other metabolically active markers. Potentially, with a more complete model of NADH bleaching and production in these types of experiments, the approach to steady state alone in an imaging experiment may provide additional information on NADH production.

One of the most important facets of ED-FRAP is that it can provide significantly more information than steady-state metabolite measurements usually obtained in conventional studies. Steady-state measurements of metabolite fluorescence are complicated by the inability to correlate mechanism to the observed concentration changes. For instance, an increase in cellular NADH fluorescence could be a function of decreased NADH oxidation or increased NAD^+ reduction by metabolism. In contrast, an increase in ED-FRAP rates of recovery must be ascribed to either an increase in dehydrogenase activity and/or increases in rate limiting substrate concentrations in the region of the enzyme. Thus, ED-FRAP provides much more information than the determination of concentration alone.

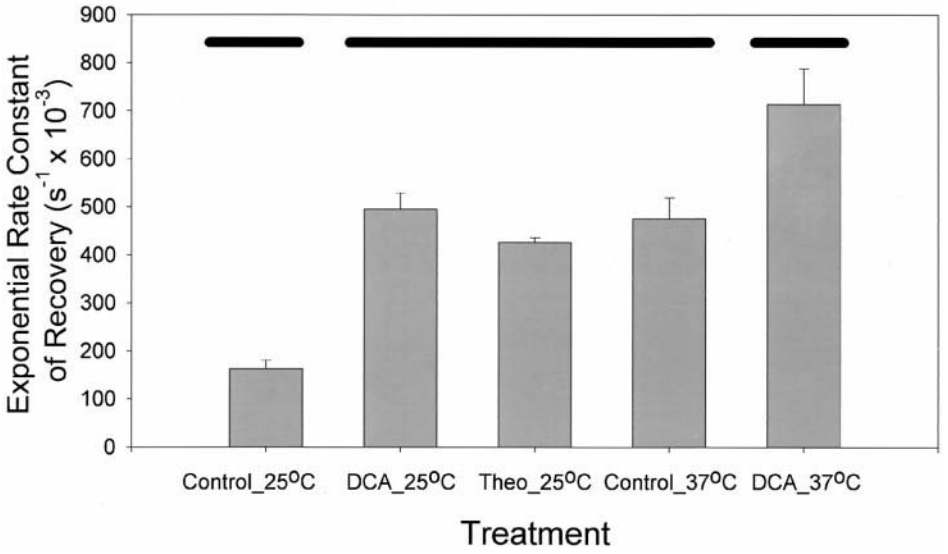

FIGURE 8 The NADH recovery exponential rate constant is temperature- and dehydrogenase activity level-sensitive in cardiac myocytes. Mean and SEM values for the exponential rate constant (averaged over the entire cell volume) of recovery after photobleaching versus treatment for superfused cardiac myocytes. Control at the two temperatures stands for superfusion rates of >3 ml/min with nutrient medium (n = 11 and 12 at 25 and 37°C, respectively). DCA at the two temperatures stands for superfusion with 5 mM DCA and 5 mM pyruvate added to the nutrient medium (n = 5 at each temperature). Theo 25°C stands for superfusion with theophylline (17 μg/ml). The combination of DCA and pyruvate is reported as a potent stimulator of dehydrogenase activity. The lines at the top of the panel indicate significant differences in mean values between treatments (ANOVA, Tukey, $p < 0.05$).

As discussed earlier, these data are consistent with the notion that k_{NADH} from ED-FRAP of NADH in cardiac myocytes is correlated with mitochondrial dehydrogenase activity based on its localization in the mitochondria. However, it is unclear which mitochondrial dehydrogenase system(s) contributes to the NADH recovery rate. Based on in vitro activity measurements (Table 1) many dehydrogenases could contribute to the ED-FRAP rate. Based on these activities determined in vitro, malate dehydrogenase has the largest activity and can enhance the fluorescence of NADH (Jameson et al., 1989). However, DCA and theophylline were found to increase k_{NADH} ~3-fold at 25°C in this study. DCA and cAMP have been shown to activate pyruvate dehydrogenase (PDH) (Sugden and Holness, 1994; Bersin and Stacpoole, 1997). These data suggest that PDH may also play an important role in NADH ED-FRAP despite its low in vitro activity (Table 1). These hormone effects could also be affecting the net flux through several upstream and downstream metabolic steps kinetically via substrate and product concentrations, as well as a variety of allosteric effects. Thus, localizing these effects to one dehydrogenase system is difficult. The reciprocal effects of NADH photobleaching on FAD^+ (Fig. 7) suggest that ED-FRAP is interrogating an NADH pool enzymatically coupled to the FAD^+/FADH system, implying that the pool is in general metabolic communication within the matrix and not an isolated pool. Though more work will be required to identify the specific enzymes and bound pools of NADH participating in the ED-FRAP reaction, it is apparent that ED-FRAP is monitoring one aspect of the delivery of the primary energy source, NADH reducing equivalents, to the electron transport system.

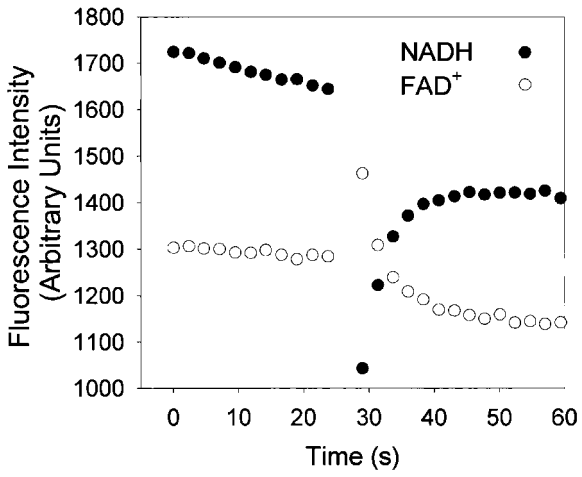

FIGURE 9 Dual acquisition of NADH and FAD^+ autofluorescence reveals inverse metabolic coupling with NADH bleaching. Plot of NADH (*open circles*) and FAD^+ (*closed circles*) fluorescence intensity over time from a single cardiac myocyte. The drop in NADH fluorescence around 29 s is due to the photobleaching pulse (at 351 nm) that is selective for NADH. The FAD^+ (flavin adenine nucleotide) signal (excitation 488 nm, emission 520 nm (Chance et al., 1972) increases immediately after the NADH photobleaching. Intensity values are the mean of all pixel values greater than the signal from the nucleus.

Given these considerations it is clear that ED-FRAP could contribute to the understanding of the cellular regulatory processes involved in energy metabolism in living

TABLE 1 Mitochondrial enzyme activities obtained from the literature for rat cardiac muscle

Enzyme	Assay Temperature (°C)	Activity (U/g wet weight)	Reference
Malate dehydrogenase	25	405	Shonk and Boxer, 1964
Isocitrate dehydrogenase	30	155*	Poston and Parenteau, 1992
3-Hydroxyacyl-coenzyme A dehydrogenase	37	81	Zonderland et al., 1999
NADH dehydrogenase (complex 1)	30	35†	Genova et al., 1995
Succinate dehydrogenase	25	6*	Link et al., 1998
Pyruvate dehydrogenase	30	5	Seymour and Chatham, 1997
α-Ketoglutarate dehydrogenase	25	3†	Lucas and Szweda, 1999
Glutamate dehydrogenase	25	1*	Adisa and Odutuga, 1998

*Converted from U/mg protein in homogenized to U/g wet weight by multiplication by 140 mg protein/g wet weight (Balaban et al., 1996).
†Converted from U/mg mitochondrial protein by multiplication by 36 mg mitochondrial protein/g wet weight (Balaban et al., 1996).

cells in ways that were previously not possible. Reducing equivalent delivery is likely a critical factor in the regulation of oxidative phosphorylation in the heart via the modification of the maximum ATP production rate (Hansford, 1980; Balaban, 1990). Additionally, ED-FRAP may play an important role in examining the relationship between Ca^{2+} and dehydrogenase activity within living cells, which has been shown to have a large impact on substrate utilization and ATP production in isolated mitochondria (Hansford, 1980). This may be particularly relevant in regard to determining the importance of the association of mitochondria with other intracellular organelles, like the sarcoplasmic reticulum, that histological studies have shown varies regionally (Scales, 1983; Shimada et al., 1984). Recent studies have shown that these associations may play a critical role in calcium buffering and sequestration (Rutter and Rizzuto, 2000). Studies have also suggested a metabolic difference between different cellular pools of heart mitochondria, such as the subsarcolemma and intrafibrillar mitochondria (Palmer et al., 1985). Again, ED-FRAP may provide a direct evaluation of these proposed metabolic differences within an intact cell.

ED-FRAP measurements may not be limited to NADH linked reactions alone. We have already shown that even indirect responses to the photobleaching can be detected in FAD^+-linked reactions (see Fig. 8). In addition, specific fluorescence markers of enzymatic modifications of metabolites could be used to monitor other reaction mechanisms inside cells. In these applications, the substrates must be converted between a fluorescent species and a molecule with different absorption and fluorescence spectral properties to selectively eliminate a product or a substrate using the photobleaching approach. If exogenous tracer probes are used, the effect of bleaching on probe concentration will not be as critical as naturally occurring metabolites like NADH or FAD^+.

In summary, we have demonstrated that NADH ED-FRAP provides a new tool for unraveling the role of NADH generation in the regulation of mitochondria ATP production, as well as potential new insights into complexities of cellular compartmentation in this process.

We thank Drs. Anthony Aletras and Han Wen for many useful discussions and assistance in IDL programming. We also thank Stephanie French and Raimundo Correa for preparation of porcine mitochondria and rabbit ventricular myocytes, respectively.

REFERENCES

Adisa, A. O., and A. A. Odutuga. 1998. Changes in the activities of three diagnostic enzymes in the heart of rats following the consumption of diets deficient in zinc and essential fatty acids. *Biochem. Mol. Biol. Int.* 46:571–576.

Axelrod, D., D. E. Koppel, J. Schlessinger, E. Elson, and W. W. Webb. 1976. Mobility measurement by analysis of fluorescence photobleaching recovery kinetics. *Biophys. J.* 16:1055–1069.

Balaban, R. S. 1990. Regulation of oxidative phosphorylation in the mammalian cell. *Am. J. Physiol. Cell Physiol.* 258:C377–C389.

Balaban, R. S., V. K. Mootha, and A. A. Arai. 1996. Spectroscopic determination of cytochrome c oxidase content in tissues containing myoglobin or hemoglobin. *Anal. Biochem.* 237:274–278.

Barman, T. E. 1969. Enzyme Handbook. Springer-Verlag, New York.

Bersin, R. M., and P. W. Stacpoole. 1997. Dichloroacetate as metabolic therapy for myocardial ischemia and failure. *Am. Heart J.* 134:841–855.

Chacon, E., J. M. Reece, A. L. Neiminen, G. Zahrebelski, B. Herman, and J. L. Lemasters. 1994. Distribution of electrical potential, pH, free Ca^{2+}, and volume inside cultured adult rabbit cardiac myocytes during chemical hypoxia: a multiparameter digitized confocal microscopic study. *Biophys. J.* 66:942–952.

Chance, B., I. A. Salkovitz, and A. G. Kovach. 1972. Kinetics of mitochondrial flavoprotein and pyridine nucleotide in perfused heart. *Am. J. Physiol.* 223:207–218.

Depre, C., S. Ponchaut, J. Deprez, L. Maisin, and L. Hue. 1998. Cyclic AMP suppresses the inhibition of glycolysis by alternative oxidizable substrates in the heart. *J. Clin. Invest.* 101:390–397.

Eng, J., R. M. Lynch, and R. S. Balaban. 1989. Nicotinamide adenine dinucleotide fluorescence spectroscopy and imaging of isolated cardiac myocytes. *Biophys. J.* 55:621–630.

Erecinska, M., D. F. Wilson, and K. Nishiki. 1978. Homeostatic regulation of cellular energy metabolism: experimental characterization in vivo and fit to a model. *Am. J. Physiol. Cell Physiol.* 234:C82–C89.

Genova, M. L., C. Castelluccio, R. Fato, C. G. Parenti, P. M. Merlo, G. Formiggini, C. Bovina, M. Marchetti, and G. Lenaz. 1995. Major changes in complex I activity in mitochondria from aged rats may not be detected by direct assay of NADH:coenzyme Q reductase. *Biochem. J.* 311:105–109.

Hansford, R. G. 1980. Control of mitochondrial substrate oxidation. *Curr. Top. Bioenerg.* 10:217–278.

Hochachka, P. W., and G. N. Somero. 1984. Biochemical Adaptation. Princeton University Press, Princeton, NJ.

Icenogle, R. D., and E. L. Elson. 1983. Fluorescence correlation spectroscopy and photobleaching recovery of multiple binding reactions. I. Theory and FCS measurements. *Biopolymers.* 22:1919–1948.

Jameson, D. M., V. Thomas, and D. M. Zhou. 1989. Time-resolved fluorescence studies on NADH bound to mitochondrial malate dehydrogenase. *Biochim. Biophys. Acta.* 994:187–190.

Kunz, W. S., and W. Kunz. 1985. Contribution of different enzymes to flavoprotein fluorescence of isolated rat liver mitochondria. *Biochim. Biophys. Acta.* 841:237–246.

Link, G., A. Saada, A. Pinson, A. M. Konijn, and C. Hershko. 1998. Mitochondrial respiratory enzymes are a major target of iron toxicity in rat heart cells. *J. Lab. Clin. Med.* 131:466–474.

Lowry, O. H., and J. V. Passonneau. 1972. A flexible system of enzymatic analysis. Academic Press, New York.

Lucas, D. T., and L. I. Szweda. 1999. Declines in mitochondrial respiration during cardiac reperfusion: age-dependent inactivation of alpha-ketoglutarate dehydrogenase. *Proc. Natl. Acad. Sci. USA.* 96: 6689–6693.

McCormack, J. G., A. P. Halestrap, and R. M. Denton. 1990. Role of calcium ions in regulation of mammalian intramitochondrial metabolism. *Physiol. Rev.* 70:391–425.

Nagai, Y., M. Miyazaki, R. Aoki, T. Zama, S. Inouye, K. Hirose, M. Iino, and M. Hagiwara. 2000. A fluorescent indicator for visualizing cAMP-induced phosphorylation in vivo. *Nat. Biotechnol.* 18:313–316.

Nuutinen, E. M. 1984. Subcellular origin of the surface fluorescence of reduced nicotinamide nucleotides in the isolated perfused rat heart. *Bas. Res. Card.* 79:49–58.

Palmer, J. W., B. Tandler, and C. L. Hoppel. 1985. Biochemical differences between subsarcolemmal and interfibrillar mitochondria from rat cardiac muscle: effects of procedural manipulations. *Arch. Biochem. Biophys.* 236:691–702.

Patel, M. S., and T. E. Roche. 1990. Molecular biology and biochemistry of pyruvate dehydrogenase complexes. *FASEB J.* 4:3224–3233.

Poston, J. M., and G. L. Parenteau. 1992. Biochemical effects of ischemia on isolated, perfused rat heart tissues. *Arch. Biochem. Biophys.* 295: 35–41.

Romashko, D. N., E. Marban, and B. O'Rourke. 1998. Subcellular metabolic transients and mitochondrial redox waves in heart cells. *Proc. Natl. Acad. Sci. USA.* 95:1618–1623.

Rutter, G. A., and R. Rizzuto. 2000. Regulation of mitochondrial metabolism by ER Ca^{2+} release: an intimate connection. *Trends. Biochem. Sci.* 25:215–221.

Saks, V. A., Y. O. Belikova, and A. V. Kuznetsov. 1991. In vivo regulation of mitochondrial respiration in cardiomyocytes: specific restrictions for intracellular diffusion of ADP. *Biochim. Biophys. Acta.* 1074:302–311.

Scales, D. J. III. 1983. Three-dimensional electron microscopy of mammalian cardiac sarcoplasmic reticulum at 80 kV. *J. Ultrastruct. Res.* 83:1–9.

Seymour, A. M., and J. C. Chatham. 1997. The effects of hypertrophy and diabetes on cardiac pyruvate dehydrogenase activity. *J. Mol. Cell Cardiol.* 29:2771–2778.

Shimada, T., K. Horita, M. Murakami, and R. Ogura. 1984. Morphological studies of different mitochondrial populations in monkey myocardial cells. *Cell Tissue Res.* 238:577–582.

Shonk, C. E., and G. E. Boxer. 1964. Enzyme patterns in human tissue. 1. Methods for the determination of glycolytic enzymes. *Can. Res.* 24: 709–721.

Smith, C. L., K. J. Zaal, and J. Lippincott-Schwartz. 1998. Looking at the bright side of photobleaching: analysis of intracellular protein dynamics by confocal microscopy. *Scanning.* 20:147–148.

Srivastava, D. K., and S. A. Bernhard. 1987. Biophysical chemistry of metabolic reaction sequences in concentrated enzyme solution and in the cell. *Annu. Rev. Biophys. Biophys. Chem.* 16:175–204.

Sugden, M. C., and M. J. Holness. 1994. Interactive regulation of the pyruvate dehydrogenase complex and the carnitine palmitoyltransferase system. *FASEB J.* 8:54–61.

Territo, P. R., V. K. Mootha, S. A. French, and R. S. Balaban. 2000. Ca^{2+} activation of heart mitochondrial oxidative phosphorylation: role of the F_0/F_1-ATPase. *Am. J. Physiol. Cell Physiol.* 278:C423–C435.

Wilson, D. F. 1994. Factors affecting the rate and energetics of mitochondrial oxidative phosphorylation. *Med. Sci. Sports Exerc.* 26:37–43.

Zonderland, M. L., P. R. Bar, J. C. Reijneveld, B. M. Spruijt, H. A. Keizer, and J. F. Glatz. 1999. Different metabolic adaptation of heart and skeletal muscles to moderate-intensity treadmill training in the rat. *Eur. J. Appl. Physiol.* 79:391–396.